

## High-Velocity Clouds in M 83 and M 51

Eric D. Miller

*Center for Space Research, Massachusetts Institute of Technology,  
Cambridge, MA 02139, USA*

Joel N. Bregman

*Department of Astronomy, University of Michigan, Ann Arbor, MI  
48109, USA*

**Abstract.** Various scenarios have been proposed to explain the origin of the Galactic high-velocity clouds, predicting different distances and implying widely varying properties for the Galaxy's gaseous halo. To eliminate the difficulties of studying the Galactic halo from within, we have embarked on a program to study anomalous neutral gas in external galaxies, and here we present the results for two nearby, face-on spiral galaxies, M 83 and M 51. Significant amounts of anomalous-velocity H I are detected in deep VLA 21-cm observations, including an extended, slowly rotating disk and several discrete H I clouds. Our detection algorithm reaches a limiting H I source mass of  $7 \times 10^5 M_{\odot}$ , and it allows for detailed statistical analysis of the false detection rate. We use this to place limits on the HVC mass distributions in these galaxies and the Milky Way; if the HVC populations are similar, then the Galactocentric HVC distances must be less than about 25 kpc.

### 1. Introduction

The high-velocity clouds (HVCs) of the Milky Way galaxy were discovered over 40 years ago by Muller et al. (1963), and have been extensively studied in H I emission, H $\alpha$  emission, and absorption, but their nature remains puzzling. These clouds of H I gas, deviating from the disk velocity by up to  $300 \text{ km s}^{-1}$ , exhibit a tremendous variation in size, morphology and velocity. The largest complexes span many degrees on the sky and possess complicated spatial structure, while the compact high-velocity clouds (CHVCs; Braun & Burton 1999) are of small angular extent. The distances to the HVCs remain largely unknown, except for a few with direct determinations (*e.g.*, absorption against background halo stars, Wakker 2001) or indirect determinations (*e.g.*, Bland-Hawthorn et al. 1998; Putman et al. 2003).

A number of formation theories posit either galactic or extragalactic origins for the HVCs, predicting different physical and dynamical properties. Among the galactic models, the most favored is the galactic fountain, a cyclic phenomenon whereby hot ( $T \sim 10^6 \text{ K}$ ) gas is ejected by supernova explosions into the lower halo, where it cools and falls back down as observable H I (Shapiro & Field 1976; Bregman 1980). Models which point to an extragalactic origin include stripping from companion galaxies, accretion from the inter-

Table 1. Predictions of HVC Production Scenarios

scenario	distance (kpc)	$ v_{\text{dev}} $ (km s <sup>-1</sup> )	size (kpc)	$M_{\text{cloud}}$ ( $M_{\odot}$ )	$Z$ ( $Z_{\odot}$ )
IGM infall	< 3	< 150	< 1	< 10 <sup>4</sup>	0.1–0.3
galactic fountain	< 10	< 150	< 1	10 <sup>4</sup> –10 <sup>5</sup>	$\geq 1$
companion stripping	5–100	< 300	$\sim 1$	10 <sup>5</sup> –10 <sup>6</sup>	0.1–1
circumgalactic DM halos	$\sim 150$	< 300	$\sim 1$	10 <sup>6</sup>	0.1–0.3
Local Group DM halos	$\sim 750$	< 300	1–10	10 <sup>8</sup>	0.1–0.3

Sizes and masses shown are typical values based on the median observed parameters of the HVC ensemble. Masses for the first three scenarios assume H I is the primary constituent of the cloud, while the mini-halo scenarios assume an H I to dark matter ratio of 0.1. Velocities for the galactic fountain and IGM infall models assume an adiabatic corona of fully ionized gas with  $T \sim 10^6$  K.

galactic medium (IGM; *e.g.*, Oort 1966, 1970, 1981), or a population of gaseous, dark-matter-dominated mini-halos, either concentrated within  $\sim 200$  kpc of our galaxy or scattered throughout the Local Group (*e.g.*, Oort 1966; Blitz et al. 1999). Since the inferred mass of a 21cm-emitting H I cloud goes as the distance squared, the mass distribution of the HVC ensemble is quite different under the various scenarios, as summarized in Table 1.

The distance and mass distributions provide fundamental demarcations for the formation scenarios, and along with metallicity they can select one or another. Mass depends on distance, however, and HVC distance is difficult to determine for clouds of primarily neutral hydrogen. This problem can be largely overcome by observing external galaxies of known distance and of similar type to the Milky Way. Evidence of anomalous H I sources in spiral galaxies has been observed for over a decade (*e.g.* van der Hulst & Sancisi 1988; Kamphuis et al. 1991; Kamphuis & Briggs 1992; Kamphuis & Sancisi 1993), and a recent study has revealed for the first time an extensive population of discrete H I clouds around an external galaxy (M31; Thilker et al. 2004).

This contribution describes the first results of a study of nearby spiral galaxies to search for HVC counterparts and other anomalous H I. Deep VLA observations of M 83 and M 51 have revealed several discrete H I sources. Comparison of the derived source mass distributions to the expected Galactic HVC distribution allows us to discriminate between the various HVC production scenarios. Full details of the analysis are presented by Miller (2003) and in papers currently in preparation.

## 2. Sample Selection and Observations

The project requires observations of large, late-type spiral galaxies located nearby to increase H I mass sensitivity and spatial resolution. Orientation effects limit the visibility of anomalous clouds; while edge-on galaxies allow discrimination of features in the galactic  $z$  direction, nothing can be known about the  $z$  velocity.

In contrast, galaxies viewed face-on reveal vertical velocity structure, but line-of-sight positions are degenerate, and high- $z$  sources merge with the disk emission if they are sufficiently low in  $z$  velocity. Inclined galaxies avoid these effects to some extent, as has been demonstrated with NGC 2403 (Fraternali et al. 2002, and elsewhere in these proceedings), although the parameter space probed is somewhat lessened. Overcoming these degeneracies requires a sample covering a range of inclinations.

We have begun this project by observing two bright, nearby, face-on spiral galaxies, M 83 and M 51. The H I 21-cm emission line observations were taken in 1999 with the VLA in D array, with a spatial resolution of about  $40''$ , an effective bandwidth of  $\pm 270 \text{ km s}^{-1}$  (centered on the systemic velocity), and a velocity resolution of  $5.2 \text{ km s}^{-1}$  after processing. The primary beam HPBW of  $30'$  provided an effective field of view of diameter 40 kpc for M 83 (4.5 Mpc distant) and 75 kpc for M 51 (8.4 Mpc distant). The dirty image cubes, with effective exposure times of about 12 hr, were deconvolved with the Multi-Resolution Clean of Wakker & Schwarz (1988). Deep optical observations were taken with the Curtis Schmidt telescope (M 83, in 1999) and MDM 1.3m telescope (M 51, in 2002) to search for stellar streams associated with anomalous H I.

### 3. Large-Scale Anomalous H I

The inner regions of both galaxies exhibit H I structure and kinematics typical of spiral galaxies, with a central hole in the H I distribution and a “spider diagram” velocity map (see Figure 1). Both galaxies also contain H I well outside of the optically-defined disk, with 80% of the H I in M 83 found here (Huchtmeier & Bohnenstengel 1981) and with M 51 exhibiting long arcs of H I emission unassociated with starlight (see also Rots et al. 1990). While these are extreme cases, spiral galaxies often possess extended disks of H I.

Removal of the thin, kinematically cold H I disk is helpful in searching for anomalous material. We did this by fitting a Gaussian to the peak of the velocity profile along every line-of-sight in the data cube and subtracting this model. The residual cube contained H I projected on the disk but at much different velocities, as well as H I emission found in the wings of the disk profile. A position-velocity ( $p$ - $v$ ) cut for the full M 83 data cube and the residual cube is shown in Figure 2 with the slice taken along the major axis (as shown in Figure 1). Measurable H I is found in the residual cube at velocities between systemic and the rotation velocity. The total intensity map of the residual cube shows that this material is structured into a clumpy disk, and a map of the difference between the mean disk velocity and the mean residual H I velocity shows that it is rotating in the same sense as the thin disk, but  $40\text{--}50 \text{ km s}^{-1}$  more slowly in projection (see Figure 2). If the rotation axes of the two components are aligned, then the anomalous H I is rotating at about  $100 \text{ km s}^{-1}$ , or half the speed of the thin disk. The total H I mass of this extended feature is  $6 \times 10^7 M_{\odot}$ , about 1% of the total H I mass of the galaxy. M 51 shows a similar anomalous disk containing about 3% of the total H I mass.

The slowly rotating anomalous H I disk is similar to features seen in NGC 891 and NGC 2403. In the former, Swaters et al. (1997) found a vertically extended layer of H I rotating  $25\text{--}100 \text{ km s}^{-1}$  more slowly than the thin disk. In

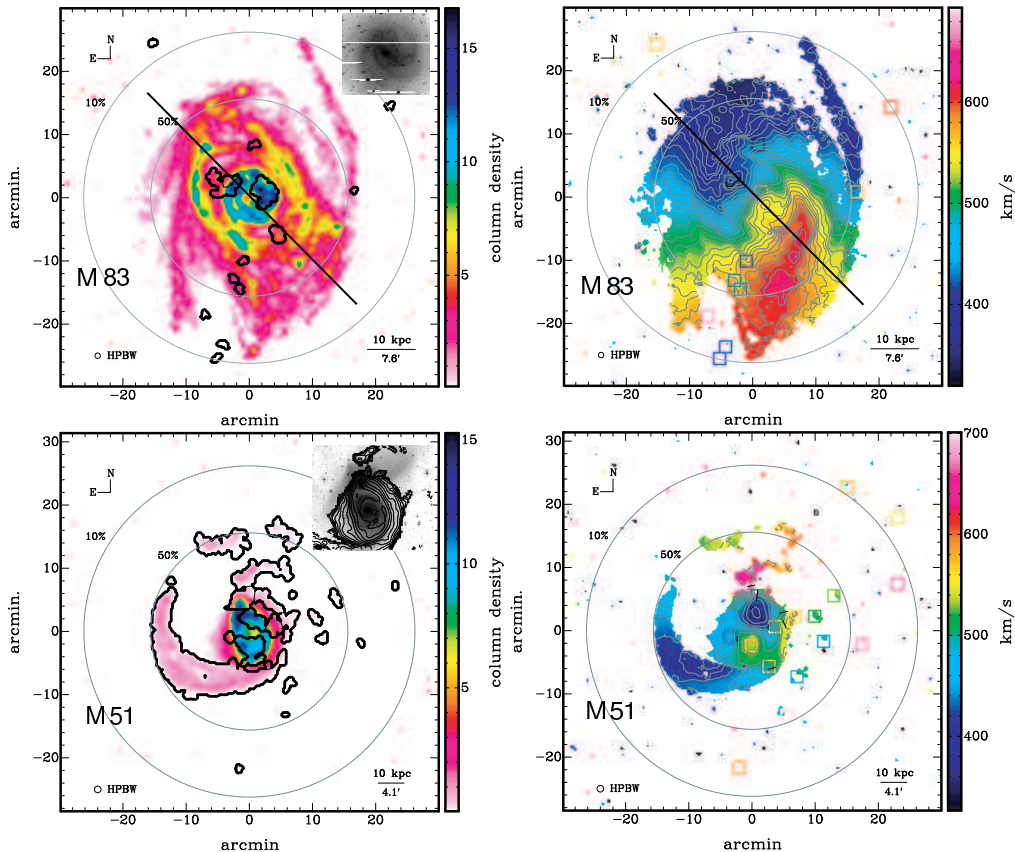


Figure 1. H I column density (in  $10^{20} \text{ cm}^{-2}$  units) and mean velocity maps for M 83 and M 51. The circles indicate the half-power and one-tenth-power widths for the primary beam. The black contours in the column density maps show the locations of the detected AVCs, while the color of the squares in the velocity maps show their velocities. Optical images are shown at the same scale. The diagonal line in the M 83 maps shows the slice taken in Figure 2.

NGC 2403, Fraternali et al. (2002) identified the “beard”, a layer of H I thought to be rotating  $20\text{--}50 \text{ km s}^{-1}$  more slowly than the thin disk.

#### 4. Small-Scale Anomalous H I

Radio astronomy suffers from a lack of robust, statistical, 3-d source detection software. In response to this, we developed a suite of algorithms to search a data cube of semi-independent pixels (as is the case for radio synthesis imaging), borrowing heavily from the methods developed by Uson et al. (1991) and Williams et al. (1994). The software applies a matched velocity filter to the data cube, enhancing velocity features with widths similar to the filtering kernel (a Gaussian). Statistically significant peaks are identified and delineated into sources by a 3-d contouring scheme, down to some specified threshold. The

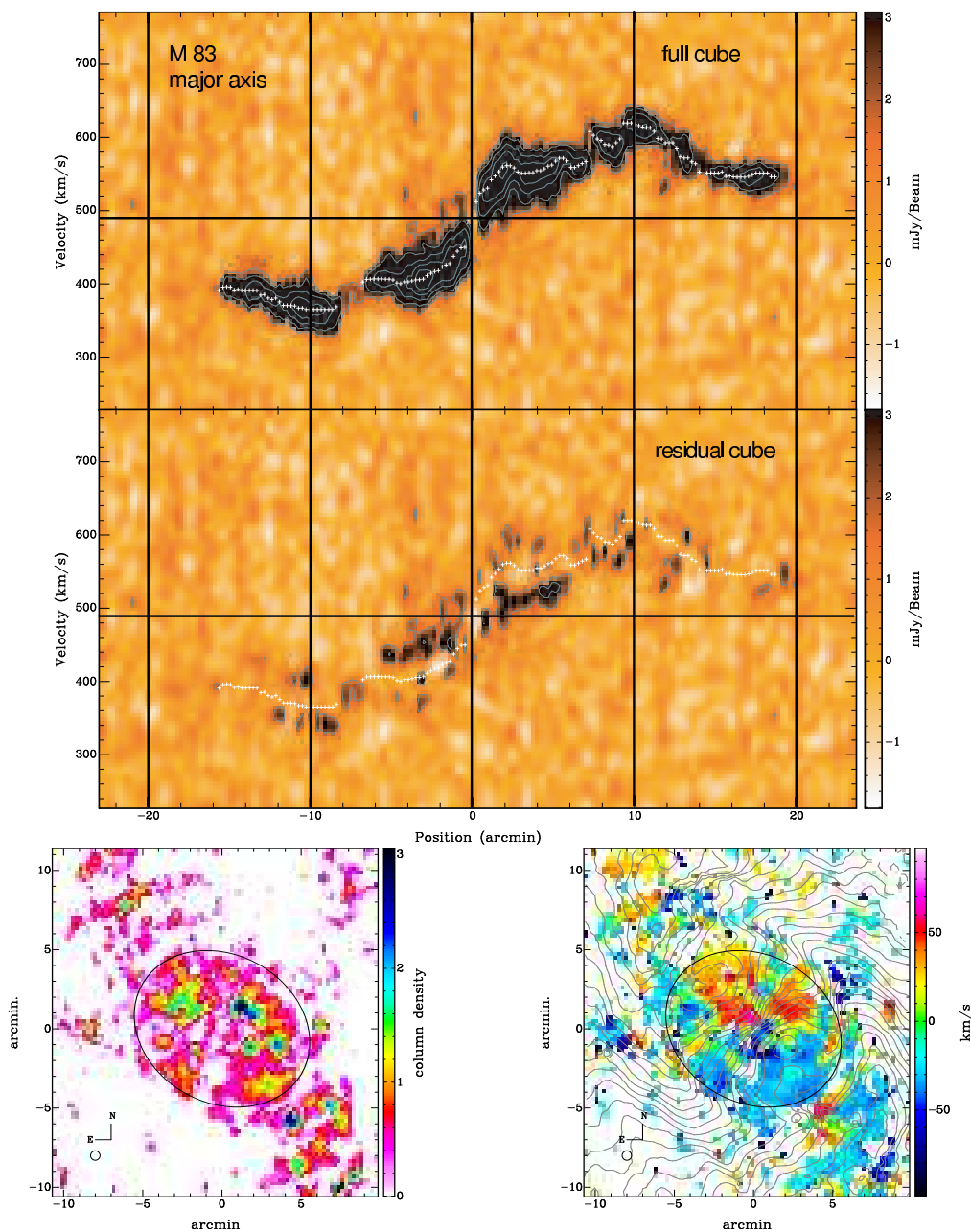


Figure 2. *Top:* Position-velocity plots for the full M 83 H I cube and the disk-subtracted cube. The residual cube contains significant emission between systemic and rotational velocity, which is traced by white crosses. *Bottom:* H I column density (in  $10^{20} \text{ cm}^{-2}$  units) and deviation velocity maps for the disk-subtracted cube of M 83. Disk-like H I emission remains, and it appears to be rotating  $40\text{--}50 \text{ km s}^{-1}$  more slowly than the thin disk in projection. The contours trace the thin H I disk velocity, in spacings of  $10 \text{ km s}^{-1}$ , to show its orientation and extent. The ellipse traces the inner stellar disk.

bright H I disk is subtracted and/or masked to prevent detection of the profile wings.

Using this technique, we discovered 14 anomalous-velocity clumps (AVCs) in M 83 and 23 AVCs in M 51. These discrete emission sources, shown in Figure 1, range from being unresolved to spanning several synthesized beams. Some are projected over the stellar disk (typically the extended ones), while some are found in regions free of starlight down to 27 R magnitudes per square arcsec (typically the compact ones, although M 51 has several large H I features at large radii). The H I masses are calculated from the 21-cm luminosities, and these range from  $5 \times 10^5$  to  $1 \times 10^8 M_\odot$  with most in the  $10^6 M_\odot$  range. The deviation velocities range from  $50 \text{ km s}^{-1}$  (the lowest we can detect) to  $200 \text{ km s}^{-1}$ .

Some of these detections are likely spurious, and we can use the detection algorithm to determine the completeness and false discovery rate with simulated datasets. Using noise and data cube characteristics similar to the real data, we simulated 9000 sources of nine different H I masses and processed them with the detection software. All sources were detected down to a mass of  $6 \times 10^5 M_\odot$  assuming a distance for M 83 ( $2 \times 10^6 M_\odot$  for M 51). We constructed 400 data cubes of Gaussian noise and processed them with the software to obtain the false discovery rate. Several spurious sources were detected below  $1 \times 10^6 M_\odot$ , with detections above  $1.5 \times 10^6 M_\odot$  being real HVCs at the 95% confidence level for M 83 ( $5 \times 10^6$  for M 51). Three of the 14 AVCs in M 83 and 15 of 23 AVCs in M 51 are above this threshold and likely to be real. The mass distributions of the low-mass AVCs were compared to the mass distribution of false detections with a K-S test. The M 83 AVCs were found to be consistent with spurious detections (K-S probability of 61%), while the M 51 AVCs were inconsistent with purely false detections, to the 99% confidence level (K-S probability of 1%). While nothing can be concluded about the verity of the M 83 detections, there is a statistically significant excess of low-mass sources in M 51 compared to what is expected by chance.

Knowledge of the HVC mass distribution in other galaxies allows us to constrain the mass distribution (and more importantly the spatial distribution) of the HVCs observed around our own Galaxy. We must assume the HVC population of the Milky Way is similar to these other galaxies in mass, space, and kinematics. In addition, we must assume a spatial distribution for the Galactic HVCs, and here we use a uniform spherical distribution for simplicity. Using fluxes tabulated in the all-sky HVC catalog of Wakker & van Woerden (1991), we construct expected mass distributions for a number of average HVC distances ( $\langle R \rangle$ ) by randomly assigning distances to each AVC. Four such distributions are shown in Figure 3 along with the mass distribution for the M 83 HVCs, corrected for false detections. While the errors are large, the M 83 mass distribution is consistent with that of the Milky Way HVCs only if the average HVC distance is less than 25 kpc. If the Milky Way HVCs are much further away than that, and if the population is similar to that in M 83, they would be generally more massive and we would have detected significant numbers in M 83.

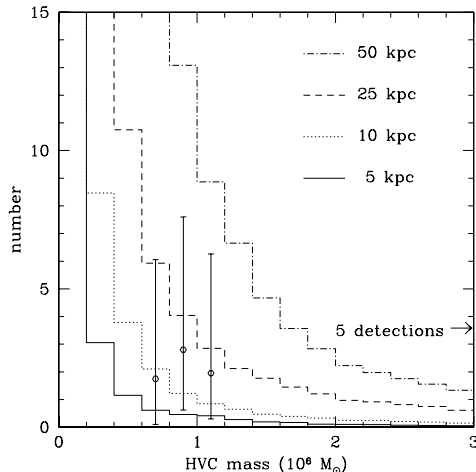


Figure 3. Mass distribution of the Milky Way HVCs, assuming uniform spherical distributions of varying mean distance and using the HVC catalog of Wakker & van Woerden (1991). The points show the false-detection-corrected distribution of our lowest-mass detections in M 83, with 95% confidence errorbars. If the HVC mass distributions of the two galaxies are similar, the Milky Way HVCs must be closer than about 25 kpc or we would have detected more HVCs in M 83.

## 5. Discussion and Interpretation

Discovery of a “beard” and limits on the HVC mass distribution in M 83 and M 51 constrain the formation models, but as one might expect, multiple scenarios remain viable, and perhaps required. Under a galactic fountain, the slowly rotating and (presumably) vertically-extended H I disk would represent condensing material beginning to fall back on to the star-forming disk. The lagging rotation is in line with expectations of the model, as material ejected from the disk would flow outward in radius and slow in rotation. A possible radial inflow discovered by Fraternali et al. (2002) in NGC 2403 supports this condensing argument as well. In addition, a simple estimate of the mass exchange rate from an assumed cooling time is  $\dot{M} \sim 1 M_{\odot} \text{yr}^{-1}$ , a value similar to the star formation rates of the galaxies under study.

The discrete H I sources are consistent with a galactic fountain. The on-disk HVCs, which are real sources of mass  $> 10^6 M_{\odot}$  in both galaxies, could be condensed, free-falling clouds or cool gas entrained in superbubbles breaking out of the galaxy. The appearance of holes in the cold H I disk at some of these locations (Miller 2003) supports the latter idea, unless the infalling clouds are sufficiently dense to punch through the disk.

Tidal stripping clearly is active in M 51, with large tidal tails of H I and streams of stars. Some of the HVC candidates to the west of M 51 might result from this as well, as it is difficult to reconcile these with a galactic fountain. The extended disk and arms of M 83 could be relics of a recent encounter, of which there is evidence in the form of a faint, arc-like optical companion (Karachentseva & Karachentsev 1998).

The other extragalactic scenarios remain viable, although this study has placed constraints on them. The anomalous H I disk could be accretion from the IGM; metallicity estimates would be invaluable to determine this. The discrete AVCs could be dark matter mini-halos, although we detect only a handful at the  $M_{\text{HI}} \sim 10^6 M_{\odot}$  level. If they are about 50 kpc from the Galaxy, we would have seen nearly five times as many detections in M 83 and M 51. Much farther than this, however, and many would have fallen outside of our field of view.

One thing made clear by this meeting is that most galaxies are found to contain “anomalous” gas upon deep observation. Warps, extended disks, and extra-planar clouds are typical of spiral galaxies, and it is the completely quiescent and regular systems that are the anomalies.

**Acknowledgments.** We wish to thank the meeting organizers, and especially Robert Braun, for engineering such an exceptional conference. Data for this project were obtained with the VLA, operated by the NRAO, a facility of the National Science Foundation operated under cooperative agreement by Associated Universities, Inc.

## References

- Bland-Hawthorn, J., Veilleux, S., Cecil, G. N., Putman, M. E., Gibson, B. K., & Maloney, P. R. 1998, *MNRAS*, 299, 611
- Blitz, L., Spergel, D. N., Teuben, P. J., Hartmann, D., & Burton, W. B. 1999, *ApJ*, 514, 818
- Braun, R. & Burton, W. B. 1999, *A&A*, 341, 437
- Bregman, J. N. 1980, *ApJ*, 236, 577
- Fraternali, F., van Moorsel, G., Sancisi, R., & Oosterloo, T. 2002b, *AJ*, 123, 3124
- Huchtmeier, W. K. & Bohnenstengel, H.-D. 1981, *A&A*, 100, 72
- Kamphuis, J. & Briggs, F. 1992, *A&A*, 253, 335
- Kamphuis, J. & Sancisi, R. 1993, *A&A*, 273, L31
- Kamphuis, J., Sancisi, R., & van der Hulst, T. 1991, *A&A*, 244, L29
- Karachentseva, V. E. & Karachentsev, I. D. 1998, *A&AS*, 127, 409
- Miller, E. D. 2003, PhD thesis, University of Michigan, Ann Arbor, Michigan
- Muller, C. A., Oort, J. H., & Raimond, E. 1963, *C. R. Acad. Sci. Paris*, 257, 1661
- Oort, J. H. 1966, *Bull. Astron. Inst. Netherlands*, 18, 421
- Oort, J. H. 1966, *A&A*, 7, 381
- Oort, J. H. 1966, *A&A*, 94, 359
- Putman, M. E., Bland-Hawthorn, J., Veilleux, S., Gibson, B. K., Freeman, K. C., & Maloney, P. R. 2003, *ApJ*, 597, 948
- Rots, A. H., Crane, P. C., Bosma, A., Athanassoula, E., & van der Hulst, J. M. 1990, *AJ*, 100, 387
- Shapiro, P. R. & Field, G. B. 1976, *ApJ*, 205, 762
- Swaters, R. A., Sancisi, R., & van der Hulst, J. M. 1997, *ApJ*, 491, 140
- Thilker, D. A., Braun, R., Walterbos, R. A. M., Corbelli, E., Lockman, F. J., Murphy, E., & Maddalena, R. 2004, *ApJ*, 601, L39
- Uson, J. M., Bagri, D. S., & Cornwell, T. J. 1991, *ApJ*, 377, L65
- van der Hulst, T. & Sancisi, R. 1988, *AJ*, 95, 1354
- Wakker, B. P. 2001, *ApJS*, 136, 463
- Wakker, B. P. & Schwarz, U. J. 1988, *A&A*, 200, 312
- Wakker, B. P. & van Woerden, H. 1991, *A&A*, 250, 509
- Williams, J. P., de Geus, E. J., & Blitz, L. 1994, *ApJ*, 428, 693